Conformation and Stability of α-Helical Membrane Proteins. 2. Influence of pH and Salts on Stability and Unfolding of Rhodopsin[†]

Reiner Vogel* and Friedrich Siebert

Biophysics Group, Institut für Molekulare Medizin und Zellforschung, Albert-Ludwigs-Universität Freiburg, Hermann-Herder-Strasse 9, D-79104 Freiburg, Germany

Received December 10, 2001; Revised Manuscript Received January 18, 2002

ABSTRACT: We studied the stability and pH-induced denaturation of rhodopsin and its photoproducts as a model for α-helical membrane proteins. The increased stability of the dark state of rhodopsin as compared to its photoproduct states allows the initiation of unfolding of the protein by light-dependent isomerization of the chromophore. We could therefore characterize the transition from the native to either acid or alkaline denatured states by light-induced Fourier transform infrared difference spectroscopy, UV−visible spectroscopy, and intrinsic tryptophan fluorescence spectroscopy. The results indicate a loss of important tertiary interactions within the protein and between the protein and the retinal chromophore in the denatured state, despite that the secondary structure of the protein is almost fully retained during the transition. We therefore propose that in this denatured state the protein adopts the conformation of a loose bundle of preserved, but only weakly interacting, transmembrane helices with a largely des-oriented and partly solvent-exposed chromophore. We further characterized the influence of salts on the stability of the rhodopsin helix bundle, which was found to follow the Hofmeister series. We found that the effect of sodium chloride may be stabilizing or destabilizing, depending on the intrinsic stability of the examined protein conformation and on salt concentration. In particular, sodium chloride is shown to counteract the formation of the denatured loose bundle state presumably by increasing the lateral pressure on the helix bundle, thereby stabilizing nativelike tertiary contacts within the protein.

Membrane proteins comprise about 30% of all proteins in eukaryotic cells (*1*), yet compared to soluble proteins only few of them are structurally characterized at a molecular level. Due to the constraints imposed by the lipid bilayer, folding and unfolding of α-helical membrane proteins are fundamentally different from the folding pathways of soluble proteins. Current models propose a sequential folding pathway for α-helical membrane proteins involving formation of secondary structural elements, presumably taking place at the membrane-solvent interface, followed by membrane insertion, and finally association of the preformed helices to the native protein (*2*, *3*). Previous studies suggested that the first step in the unfolding of membrane proteins consequently involves a loss of interhelical tertiary interactions, while secondary structure remains largely preserved (*4*). The resulting denatured state therefore corresponds to a loosely packed helix bundle.

In this study, we arrive at similar conclusions. For the first time, we investigated the pH-induced unfolding of an α-helical membrane protein by Fourier transform infrared (FTIR)[1] difference spectroscopy, which constitutes a powerful tool to examine structure−function relationships in proteins (*5*), supplemented by UV−visible and tryptophan fluorescence experiments.

As a model system, we studied the visual pigment rhodopsin, which belongs to the large family of G protein-coupled receptors and which is well characterized both by biophysical and biochemical methods (*6*−*9*). Rhodopsin consists of seven membrane-spanning helices, which are connected by cytoplasmic and extracellular loops, forming the extra-membranous cytoplasmic and extracellular domains. The unphotolyzed dark state of rhodopsin consists of the apoprotein opsin and 11-*cis* retinal, which is covalently bound to Lys-296 on helix 7 by a protonated Schiff base and buried in the receptor's transmembrane core. Activation of rhodopsin proceeds via light-dependent isomerization of the retinal chromophore from the inactive 11-*cis* to an activating all-*trans* geometry, leading ultimately to the formation of the active receptor species metarhodopsin II (Meta II) within milliseconds. This active state decays subsequently on the time scale of minutes by slow hydrolysis of the retinal Schiff base and dissociation of the receptor into opsin and free all-*trans* retinal.

The presence of 11-*cis* retinal in its binding pocket, which locks the protein in a compact inactive conformation, renders

[†] This work was supported by grants from the Deutsche Forschungsgemeinschaft (Grant VO 811/1-1 and SI 278/16-3,4) and by Fonds der Chemischen Industrie.

* Correspondence to: Reiner Vogel. Arbeitsgruppe Biophysik, Institut für Molekulare Medizin und Zellforschung, Albert-Ludwigs-Universität, Hermann-Herder-Str. 9, D-79104 Freiburg, Germany; phone +49 761 203 5391, fax +49 761 203 5390, e-mail reiner.vogel@biophysik.uni-freiburg.de.

[1] Abbreviations: FTIR, Fourier transform infrared spectroscopy; IR, infrared; Meta I and Meta II, metarhodopsin I and II; Meta II_{PSB}, metarhodopsin II with protonated Schiff base; Meta II_{380}, metarhodopsin II with deprotonated Schiff base; DM, *n*-dodecyl-β-D-maltoside; MES, 2-*N*-morpholino ethanesulfonic acid; MOPS, 3-*N*-morpholino propanesulfonic acid, BTP, bis-tris propane; TCA^-, trichloroacetate, TEA^+, tetraethylammonium.

10.1021/bi016024f CCC: $22.00
Published on Web 02/19/2002

the dark state of rhodopsin quite stable toward denaturation. In contrast to this, the photoproduct states with bound all-*trans* retinal as well as the retinal-free apoprotein opsin are considerably less stable and thus much more susceptible to denaturation. At a fixed pH and temperature, the protein can therefore be switched to a less stable conformation by light-dependent isomerization of the chromophore. This allows the initiation of unfolding of the protein by photolysis instead of temperature or pH jumps, and allows one to follow the unfolding reaction sensitively by light-induced UV−visible and FTIR difference spectroscopy.

In our study, we observed dramatic changes in the tertiary structure of the protein during the unfolding reaction, which were detected by intrinsic reporter groups in the membrane-embedded core of the protein. These are accompanied by a large reorientation of the chromophore within the protein. As compared to the extent of these considerable structural changes, however, the IR difference bands in the amide I and amide II range are very small. The amplitudes of these difference bands, which are a measure for the involved changes of the protein's secondary structure during the denaturation process, cover only about 1% of the absolute amide band absorption. We can therefore conclude that the secondary structure of the protein is almost fully preserved during this denaturation step, despite that important tertiary contacts within the protein are obviously lost. The resulting denatured loose bundle state seems to be a common unfolding product of helical membrane proteins (*2*, *10*), and may in some way correspond to the molten globule state of soluble proteins (*11*).

The second part of this study focuses on the action of salts, which are shown to have a considerable impact on the stability of the rhodopsin helix bundle. The observed ion selectivity clearly follows the so-called Hofmeister series (reviewed in refs *12*−*14*), which is a classification of ions with regard to their influence on general properties of proteins and other compounds in aqueous solution. At the advent of protein biochemistry, the salting-out of proteins by so-called Hofmeister salts was the method of choice for protein purification, and therefore mainly the solubility of proteins was investigated for practical reasons (*15*). Later, other properties, such as enzyme function and protein stability, were examined, and salts were characterized as chaotropes or destabilizers at the one end of the Hofmeister series and as kosmotropes or stabilizers at the other end. In the order of chaotropicity, the series follows $SCN^- > I^- > Br^- > Cl^- > F^- > SO_4^{2-}$ for some typically examined anions.

As already stated in the accompanying paper in this issue (*16*), there are only few studies addressing the effects of salts on the stability of membrane proteins. An influence of salts was reported previously on the photocycle kinetics of the archaeal proton pump bacteriorhodopsin (*17*), which was analyzed in terms of stochastic fluctuations of free energy barriers (*18*), and on the stability of the synthetic visual pigment 9-demethyl rhodopsin (*19*, *20*). In this study, we examined the influence of salts on the detergent-solubilized helix bundle of rhodopsin in three conformational states of differing stability. We observed the interesting phenomenon that the null point, which divides destabilizing from stabilizing salts, depends on the intrinsic stability of the protein under the respective experimental conditions.

EXPERIMENTAL PROCEDURES

Preparation of the Pigment. Bovine rhodopsin in washed disk membranes was prepared from the rod outer segments of cattle retinae after established methods (*21*). Rhodopsin was used either directly in this native membrane environment or after solubilization and purification in *n*-dodecyl-β-D-maltoside (DM, Biomol, Hamburg, Germany) by concanavalin A affinity chromatography (Pharmacia, Uppsala, Sweden) (*22*). All experiments were performed under dim red light. Pigment was stored in distilled water at −20 °C at a concentration of 30 to 50 μM.

FTIR Spectroscopy. FTIR spectroscopy was performed with 4 μm sandwich samples in transmission mode as described in the accompanying paper in this issue (*16*). These sandwich film samples, which involve a drying step on the IR windows, show a sustained preferential orientation of the disk membrane parallel to the window plane also after full hydration. IR samples of purified rhodopsin in detergent, were prepared similar as membrane samples, yet with only 0.5−0.7 μL of 200 mM buffer to prevent the sample from being washed off the window. The pH in these IR detergent samples is therefore less precisely defined than in the membrane samples.

UV−Visible Spectroscopy. UV−visible spectroscopy was performed with a thermostated Perkin-Elmer Lambda 17 UV−vis spectrophotometer either with sandwich samples identical to those used for IR spectroscopy or in 100-μL microcuvettes with 10-mm path length (Hellma, Müllheim, Germany). Photolysis of the sample was achieved by a 20-s illumination through a fiber optic and a >530 nm long-pass filter fitted to a 150 W slide projector. For measurements on diluted membrane suspensions (~2 μM) an identical, but bleached, sample was used in the reference beam to account for the considerable light scattering. Measurements with purified rhodopsin in detergent were generally performed in 0.1% DM (w/v). Scanning speed was 960 nm/min allowing for a time resolution of 1 min.

The stability of Meta II in detergent micelles was assayed with purified rhodopsin (typically 1 μM) in 0.1% DM at 20 °C in 20 mM citrate buffer, pH 3.5, supplemented with 10 mM NaSCN to shift the Meta II Schiff base protonation equilibrium entirely to Meta II_{PSB} (*23*). Meta II was formed by illumination of the dark pigment and the subsequent decay was followed by consecutive recordings of spectra in 1-min intervals.

Stability of the dark state against acid denaturation was assayed with purified rhodopsin (typically 1 μM) in 0.1% DM at 10 °C in 20 mM MOPS, pH 7.0. The reaction was started by adding in the dark 1% (v/v) 10 M HCl to the thermostated sample in the cuvette and followed by the recording of spectra in 1-min intervals. At the end of each experiment, the sample was illuminated to allow rapid denaturation of the less stable photoproduct and to determine the total pigment absorption for normalization.

Hydroxylamine reactivity of the dark state was assayed with purified rhodopsin (typically 1 μM) in 0.1% DM at 50 °C in 100 mM MOPS, pH 7.0, supplemented with 50 mM hydroxylamine. The experiments were started by addition of the pigment to the thermostated buffer solution into the cuvette and followed by spectral recordings in 1 or 4 min intervals, all in the dark. At the end of each experiment, the

sample was fully bleached by illumination to determine the total pigment absorption for normalization.

Fluorescence Spectroscopy. Fluorescence experiments were performed with a home-build thermostated fluorescence photometer. Tryptophan fluorescence was excited by a deuterium lamp fitted to an interference filter with transmission at (295 ± 5) nm, emission was recorded with a >335 nm long-pass filter in photon-counting mode.

RESULTS

Decay of Meta II in Native Membranes. Upon light activation, rhodopsin in its native membrane environment forms the active receptor species Meta II under appropriate conditions within milliseconds. This active photoproduct state decays subsequently within minutes by hydrolysis of the retinal Schiff base and dissociation of the receptor into the apoprotein opsin and all-*trans* retinal. As reported previously, the final decay product opsin is found in a conformational equilibrium between an inactive species formed at neutral to alkaline pH and an active species formed at low pH (*24*). The p*K* of this pH-dependent equilibrium of the Meta II decay product is around 4.3 at 30 °C, and the conformation of the active opsin species was found to be very similar to that of the active Meta II state. Correspondingly, we observe in the IR at pH 4.0 and 30 °C only minor changes between the spectrum of the Meta II photoproduct obtained immediately after illumination and that of opsin in the conformation being stably formed after full decay of the Meta II photoproduct at $t = 20'$ (Figure 1A).

This native conformation of opsin is obviously not stable at pH 3.5 (Figure 1B). At this pH, we observe the slow rise of IR difference bands in the amide range between 1500 and 1700 cm^{-1}, which are distinctly different from those in Meta II or in the opsin states obtained at pH 4.0 or higher. This decay to an apparently denatured state is considerably accelerated at still lower pH, and we observe at pH 2.5 a similar photoproduct already immediately after illumination (Figure 1C). As evident from the inset in Figure 1C, formation of this state in the IR is paralleled by formation of a slowly decaying 440 nm photoproduct species in the UV−visible. The dark state of rhodopsin was stable over the entire tested pH range down to pH 2.5 as evident from the unchanged visible absorption peak at 500 nm.

In rhodopsin and its photoproducts with protonated Schiff base, the wavelength of the absorption maximum is tuned from 440 nm for a protonated retinal Schiff base in solution to values between 470 and 570 nm. This shift is induced by tight tertiary interactions between the chromophore and the amino acid side chains lining the retinal binding pocket (*6*, *25*) and between the protonated Schiff base in particular and its negative counterion, Glu-113 (*26*, *27*), and is termed *opsin shift*. A 440 nm species, as obtained in our experiments after photolysis of rhodopsin at pH 2.5, is generally obtained after acid denaturation of intact rhodopsin pigments. As it lacks the opsin shift of functional pigments, it is commonly interpreted as a denatured protein state with a solvent-exposed, titratable Schiff base devoid of intimate protein−chromophore interactions. In the following section, we will try to characterize this denatured species in more detail.

Characterization of the 440 nm Species. In the IR, striking features of the 440 nm species are the difference bands in

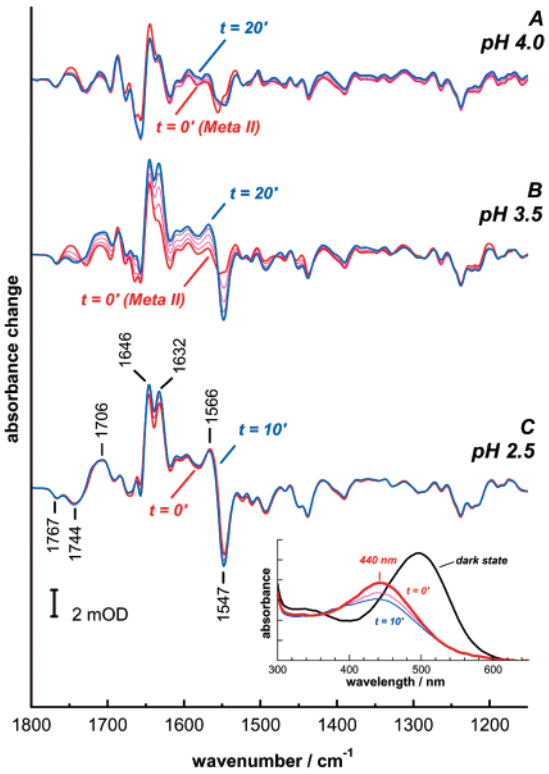

FIGURE 1: FTIR difference spectra "photoproduct minus dark state" of the rhodopsin photoproducts in disk membranes at low pH. Rhodopsin was photolyzed at pH 4.0, 3.5, and 2.5, and the temporal decay of the less stable photoproducts was followed at 30 °C. At pH 4.0 (A), the initially formed Meta II photoproduct (red) decays by hydrolysis of the Schiff base to a stable and conformationally similar opsin state (blue). At pH 3.5 (B), native Meta II is formed initially as above (red), but the opsin decay product is no longer conformationally stable and instead slowly adopts a denatured fold (blue). At pH 2.5 (C), we observe no native Meta II state after illumination. Instead, already initially a denatured state is formed with characteristic, temporally stable difference bands in the amide I and amide II range around 1650 and 1550 cm^{-1}, respectively, and in the range of protonated carboxylic acids above 1700 cm^{-1}. The inset shows the 440 nm absorption of this state in the UV−visible recorded from an identical sample at pH 2.5. All spectra were recorded in 5-min intervals.

the amide I and II range around 1650 and 1550 cm^{-1} shown in Figure 1C, of which particularly the 1632 (+) and the 1547 cm^{-1} (−) bands are clearly absent in Meta II. If we compare the intensity of the amide difference bands of the 440 nm species with those of Meta II, we find that they have roughly the same intensity. As compared to the total absorption of our samples in the amide I range of approximately 0.6 OD units (not shown), the integrated amide difference bands of Meta II comprise less than 1% of the total absorption, in agreement with previous results (*28*). Importantly, for the 440 nm species, this value is still about 1%. As shape and intensities of the amide I bands are sensitive indicators for the presence of secondary structural elements in a protein, obviously most of the secondary structure of the protein must be preserved during the transition from the dark state and even more from Meta II to the 440 nm species.

In addition to the changed bandpattern in the amide range, the pattern above 1700 cm^{-1} is different for the 440 nm species as compared to Meta II. Bands in this range reflect the stretching modes of lipid carbonyls and of protonated carboxylic acids. In the case of Meta II, the distinct band

pattern in this range was assigned to changes in the hydrogen bonding properties of membrane embedded Asp-83 and Glu-122, shifting their absorption from 1767 and 1734 cm^{-1} to an overlapping band absorbing between 1745 and 1750 cm^{-1} (*29*, *30*). This band pattern is superimposed by a smaller difference band at 1744 (+)/1727 cm^{-1} (−) due to changed interaction of the protein with lipid carbonyls in Meta II (*31*, *32*). The distinct positive band at 1712 cm^{-1} was shown to reflect the protonation of the Schiff base counterion of the dark state, Glu-113, in Meta II (*33*). In the difference spectrum of the 440 nm species, the lack of a positive band in the range around 1750 cm^{-1} is therefore best explained with a downshift of the C═O stretch mode of Asp-83 and Glu-122 to a broad absorption band around 1706 cm^{-1}, indicating a change from a weakly to a strongly hydrogen-bonding environment. IR difference spectra with similar patterns in the amide I and II range and in the range above 1700 cm^{-1} were obtained also for the salt-induced or chemical denaturation of the rhodopsin photoproducts (unpublished results).

Another structural marker of the 440 nm species is the orientation of the retinal chromophore. In the dark state of rhodopsin, the visible transition dipole moment of the chromophore is largely parallel to the plane of the disk membrane and changes only slightly upon transition to Meta II (*34*). In film samples of rhodopsin, which were prepared by drying and rehydration of membranes, the plane of the disk membranes and therefore also of the chromophore transition dipole moment are preferentially oriented perpendicular to the direction of the measuring beam. If the UV−visible difference spectra "Meta II minus dark state" obtained from such partially oriented film samples and from suspension samples with random pigment orientation are normalized to the absorption peak of the dark state, a slightly smaller absorption peak of Meta II in the film samples as compared to the suspension samples becomes obvious (Figure 2A, upper panel). This small absorption decrease indicates a slight des-orientation of the chromophore dipole moment out of the membrane plane during the transition to Meta II. In the case of the 440 nm species, a similar, yet much larger, absorption decrease is observed (Figure 2A, lower panel). This gives clear evidence that the preferential orientation of the chromophore in the membrane plane is considerably reduced during the transition to the 440 nm species.

We have further measured the changes of the intrinsic tryptophan fluorescence of rhodopsin during the transition to both Meta II and the 440 nm species. In the dark state, the fluorescence of the four tryptophans of rhodopsin is known to be quenched by energy transfer to the retinal chromophore (*35*). During the transition to Meta II, the fluorescence yield is initially slightly decreased, and increases subsequently considerably (Figure 2B) with a time dependence reflecting the hydrolysis of the Schiff base in Meta II and the release of the retinal chromophore from its binding pocket (*36*). During the transition to the 440 nm species, a large fluorescence increase can be observed instead already immediately after illumination, which subsequently increases further slowly, presumably again reflecting the hydrolysis of the chromophore also in this 440 nm species. This hydrolysis can be followed as a decrease of the 440 nm absorption in the inset of Figure 1. The concomitant absorption increase at 385 nm of free retinal is only very faint, which is presumably due to a preferential orientation of the dissociated retinal perpendicular to the membrane normal and thus parallel to the incident measuring beam in the oriented sandwich film sample. Likely, the strong initial fluorescence increase in the 440 nm species can be explained by a decreased efficiency of fluorescence energy transfer

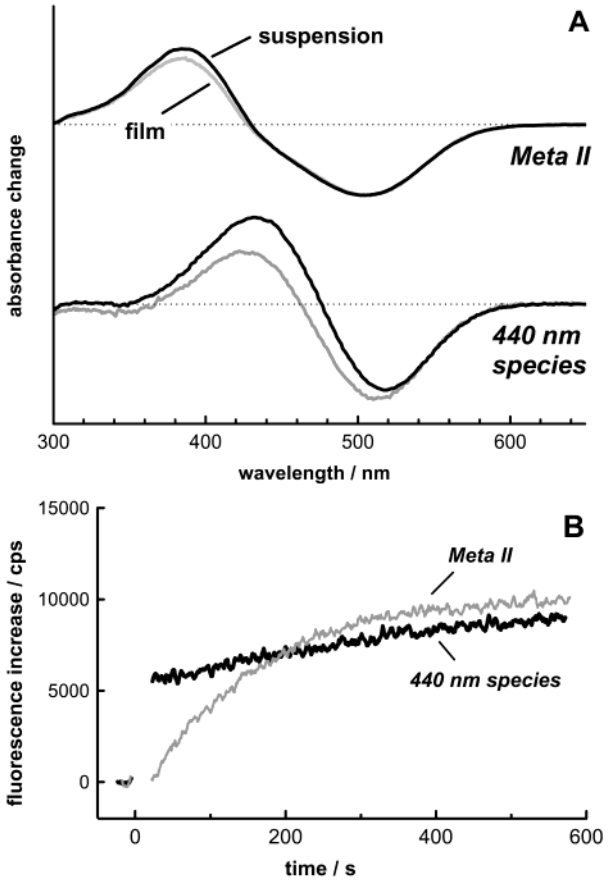

FIGURE 2: (A) Orientational change of the chromophore in the 440 nm species in comparison to Meta II. UV−visible difference spectra "photoproduct minus dark state" were recorded for the Meta II photoproduct (pH 5.0) and for the 440 nm photoproduct (pH 2.0) at 20 °C. Experiments were performed both with membrane suspension with a random orientation of the disk membranes (black) and with partially oriented sandwich film samples (gray), with a preferential orientation of the transition dipole moment of the dark state perpendicular to the incident measuring beam. For the transition to Meta II, there is a small relative decrease of the Meta II absorption peak in the film samples as compared to unoriented suspension samples. This indicates a slight desorientation of the chromophore in Meta II out of the membrane plane, thereby decreasing its apparent absorption coefficient in the film samples. A similar, but much larger effect is observed for the 440 nm species, indicating a considerably larger movement of the chromophore out of the plane of the disk membrane during the transition to this state. To account for band overlap, the spectra were normalized by the long wavelength side of the dark state depletion peak. (B) Changes of the tryptophan fluorescence during formation and decay of Meta II (pH 4.0) and of the 440 nm species (pH 2.5), both at 30 °C in disk membranes. During the transition to Meta II, the tryptophan fluorescence is initially unchanged, and increases monoexponentially during Meta II decay to opsin due to release of the otherwise quenching chromophore out of its binding pocket. During the transition to the 440 nm species at pH 2.5, we observe instead a large initial increase of the fluorescence intensity, indicating considerably less efficient energy transfer from the tryptophans to the retinal chromophore in this species. The subsequent, slower increase of the fluorescence intensity reflects as well the slow hydrolysis of the Schiff base also in this species.

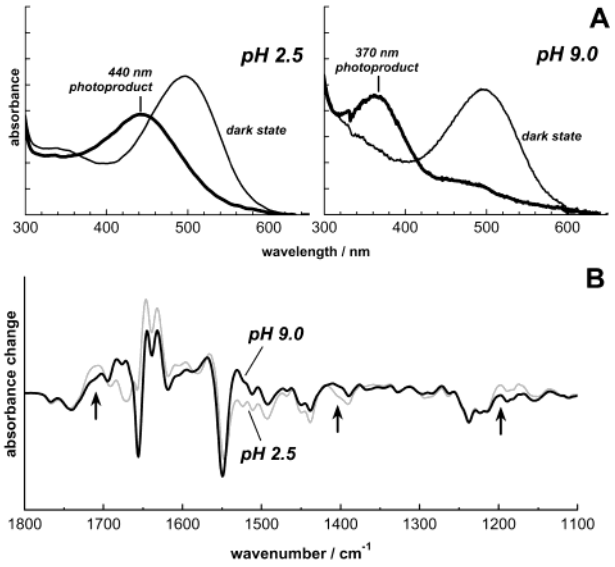

FIGURE 3: (A) UV−visible spectra of the rhodopsin photoproduct at acidic and alkaline pH. Rhodopsin in membranes was photolyzed in sandwich samples identical to those in Figure 1 at 30 °C at pH 2.5 (A) and pH 9.0 (B), and the spectra of the initial photoproducts were recorded. At both pH values, the dark state of rhodopsin showed native-like absorption at 500 nm (thin lines), while the photoproduct states (thick lines) absorbed at positions equivalent to a solvent-exposed retinal Schiff base in its protonated (440 nm) or deprotonated state (370 nm). (B) Corresponding IR difference spectra "photoproduct minus dark state" from samples identical to those in panel A. In addition to changes in the amide range, the relative absorption shift from 1706 to 1400 cm^{-1} at pH 9.0 as compared to pH 2.5 indicates a partial deprotonation of carboxylic acids during the transition to the photoproduct state at alkaline pH. The relative absorption decrease in the fingerprint range around 1200 cm^{-1} at pH 9.0 as compared to pH 2.5 reflects the deprotonated Schiff base in the photoproduct at alkaline pH, which is protonated at acidic pH.

from the tryptophans to the retinal chromophore as compared to both the dark and the Meta II state. However, contributions due to polarity changes of the immediate environment of the tryptophans may be involved as well (*35*).

Important insight into the structure of the 440 nm acid denatured species may be gained also from the study of its analogue obtained at alkaline pH. At pH 9.0, a similar denatured state is formed, which absorbs not at 440 nm, but at 370 nm, at the position expected for a solvent-exposed deprotonated Schiff base (Figure 3A). In the IR, the structural features of this state are remarkably similar to those of the 440 nm state, as shown in Figure 3B. The amide bands of the alkaline denatured state are essentially similar to those of the acid denatured state, with the exception of the region between 1650 and 1690 cm^{-1}, where there are some more pronounced changes. In the absorption range of protonated carboxylic acids above 1700 cm^{-1}, we observed at pH 2.5 a downshift of the absorption of Asp-83 and Glu-122 to values around 1706 cm^{-1}, as stated above. At alkaline pH, the broad peak at 1706 cm^{-1} is reduced, and instead we observe an absorption increase at 1400 cm^{-1}, suggesting a partial deprotonation of these membrane embedded carboxylic acids (possibly also including Glu^{113}) at pH 9.0. This is in agreement with increasing solvent exposure of these residues both in the acid and the alkaline denatured states underlining the structural similarity between these species.

We can thus summarize the main features of these denatured species as follows: (a) an absorption peak at 440 and 370 nm, respectively, indicating a solvent-exposed Schiff base and a lack of intimate tertiary contacts between protein and chromophore, (b) a change of the environment of membrane embedded carboxylic acids from weakly to strongly hydrogen-bonding, and, at alkaline pH, presumably a partial deprotonation of these groups, (c) a large orientational change of the retinal chromophore, (d) a considerably increased fluorescence from intrinsic tryptophans, and (e) only very small changes in secondary structures as judged from the amide bands. These features indicate a strong preservation of the membrane spanning helices as secondary structural elements, despite a dramatic loss of tertiary contacts between these helices and between the helices and the chromophore. The protein therefore adopts a conformation that is most appropriately described as a loose helix bundle.

Decay of Meta II in Detergent. Replacement of the native bilayer of rhodopsin by a more fluid detergent micelle is known to lead generally to a reduced stability of the protein, even for very mild detergents as dodecyl maltoside (DM) (*37*). This reduced stability in detergent becomes evident in the decay properties of Meta II. In contrast to the decay in membranes, where we observed in the range from pH 4 to pH 8 the formation of stably folded, nativelike opsin states in the IR (*24*), such stable nativelike decay products are not observed in detergent, as we will show in the following. Instead also around neutral pH, the decay product opsin eventually adopts a loose bundle-like conformation of a denatured state as it was observed in membranes only below pH 4.

In Figure 4A, we can follow the decay of Meta II in detergent at pH 5.0. As evident from the UV−visible spectra, no 440 nm species is formed, and the Meta II state, absorbing at 380 nm, decays to a 385 nm species with a half time of 3 to 4 min (determined both in solution and in sandwich samples). This absorption shift reflects the hydrolysis of the Schiff base and the release of all-*trans* retinal from its binding pocket. In the IR, we can see the slow rise of a band pattern similar as for the denatured states in membrane with a half time of about 14 min for characteristic amide bands, indicating the subsequent long-term destabilization of opsin (Figure 4A, lower panel).

An acceleration of this denaturation is observed at pH 3.0, where instead of the 380 nm species of Meta II, the 440 nm species of the still retinal bound, denatured state is formed immediately after illumination (Figure 4B, upper panel). A closer comparison of the FTIR spectrum of the loose bundle state in detergent (Figure 4B, lower panel) with that in membrane (Figure 1C) reveals quite similar difference bands in the amide II range around 1550 cm^{-1} and in the range of the protonated carboxylic acids above 1700 cm^{-1}. In the amide I range, a strong negative band at 1656 cm^{-1} is observed in detergent, which has a much smaller intensity in membrane samples. This difference is possibly a dichroitic effect, reflecting the lack of pigment orientation in the detergent film samples.

The general situation in detergent parallels therefore that in membranes, yet denaturation occurs already at less extreme pH values due to the decreased intrinsic stability of the protein in detergent micelles. In detergent at 30 °C, a general tendency of the rhodopsin photoproducts to denaturation is observed over the entire pH range, with maximal stability of the protein around pH 6 (data not shown). This observation

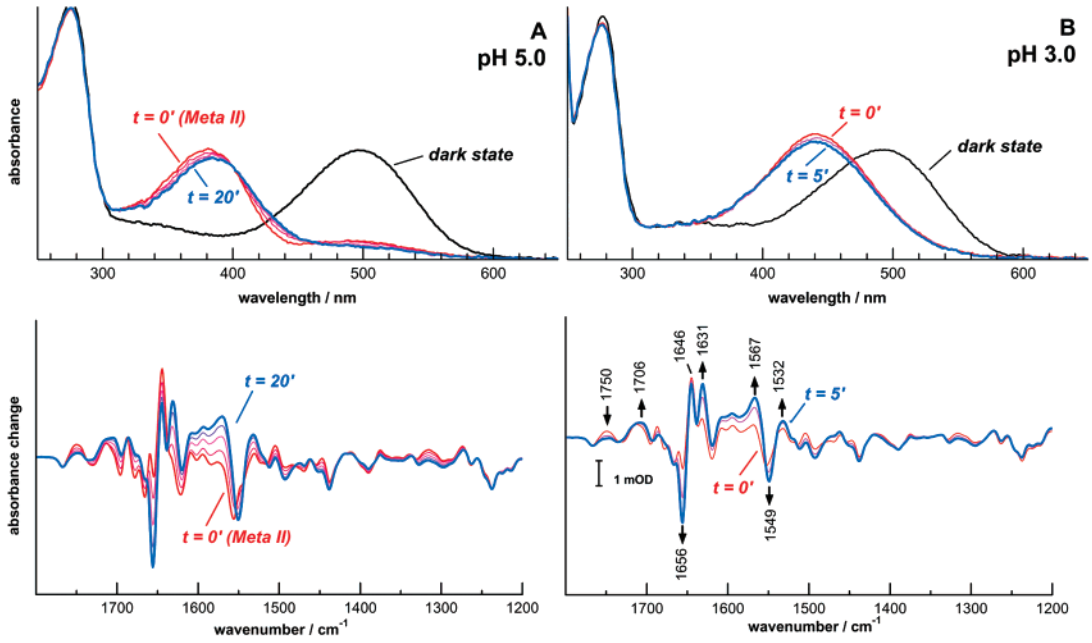

FIGURE 4: FTIR and UV−visible spectra of rhodopsin photoproducts in detergent micelles. Purified rhodopsin in dodecyl maltoside was photolyzed at 30 °C at pH 5.0 (A) and pH 3.0 (B) and the decay of the photoproducts was followed both in the UV−visible (upper panels) and in IR "photoproduct minus dark state" difference spectra (lower panels). At pH 5.0 (A), Meta II (red) decays by hydrolysis of the retinal Schiff base and dissociation of the receptor into opsin and free all-*trans* retinal (blue) as evident from the shift of the absorption peak from 380 to 385 nm with a halftime of 3−4 min. As evident from the slowly increasing IR difference bands in the amide range, the conformation of the opsin decay product is not stable at pH 5.0, but slowly adopts a denatured state conformation with a halftime of 14 min (blue). Spectra in A were recorded at $t = 0$, 5, 10, 15, and 20 min after photolysis. At pH 3.0 (B), a retinal bound 440 nm species is formed immediately after illumination, which shows characteristic IR bands of the denatured state conformation in the amide I and II range and in the range above 1700 cm^{-1}. The UV−visible spectra in panels A and B were obtained from diluted (~ 1 μM) solution samples, but are in agreement with spectra obtained from sandwich samples identical to those used for the IR experiments, which have, however, a decreased signal-to-noise ratio. Spectra in panel B were recorded at $t = 0$, 2, and 5 min after photolysis.

confirms the recent observation that opsin in detergent shows only incomplete, multiphasic regeneration kinetics upon reconstitution with 11-*cis* retinal at room temperature (*38*). These results extended previous findings of deGrip (*37*), and were interpreted as a structural instability of opsin in detergent. This leads to slow protein unfolding to non-native forms, which are either completely unable to refold to a native form and which do therefore not regenerate a functional pigment, or which may refold only slowly leading thus to very slow regeneration kinetics.

After this characterization of the rhodopsin unfolding products, we will examine in the following sections the influence of salts on different conformations of the rhodopsin helix bundle in detergent. We will start with the decay properties of Meta II under conditions where the structural stability of the protein is only marginal. We will then examine a completely destabilized acid denatured system, and finally turn to the other extreme, to the dark state at neutral pH, which is characterized by a high overall structural stability.

Influence of Salts on the Stability of Meta II in Detergent: The 385 and the 440 nm Pathway. As shown in the previous section, we observe spectroscopically two decay pathways for Meta II in detergent: Under stabilizing conditions, as, e.g., at pH 5.0, Meta II was shown to decay by hydrolysis of the Schiff base to free all-*trans* retinal, absorbing at 385 nm, and opsin. Only in the long term, with a halftime about 3 to 4 times longer, the opsin state adopts a non-native, denatured fold, which is, however, not sensed by the dissociated retinal. Under destabilizing conditions, as at pH 3.0, the protein denatures prior to hydrolysis of the Schiff base, leading thus to the formation of a retinal-bound denatured state absorbing at 440 nm. The stability of Meta II under different external conditions can therefore be conveniently analyzed by monitoring the relative contributions of the 385 and the 440 nm pathway of Meta II decay.[2]

We performed such an experiment at pH 3.5 and 20 °C, where Meta II decays both via the 385 and the 440 nm pathway, as shown in Figure 5B. At this low pH, however, the deprotonated Schiff base of Meta II, conferring it the absorption maximum at 380 nm, can easily be reprotonated from the solvent in the presence of solute anions, which were recently shown to bind to the Schiff base and to stabilize its protonated form (*23*). This anion induced protonation shifts the absorption of Meta II to 480 nm, yet without changing the active state conformation of the protein. The presence of salts of different species and concentrations will therefore inevitably lead to variable contributions of the Meta II species with protonated Schiff base, Meta II_{PSB}, to the classical Meta II with deprotonated Schiff base, Meta II_{380}. We therefore rather performed this experiment in the presence of 10 mM NaSCN, which binds to the Schiff base with high affinity, thereby increasing its p*K* to around 4.5 (*23*) and shifting at

[2] In membranes, such an analysis is hampered by the tendency of the dissociated retinal to form nonspecific Schiff bases with peripheral amino groups on the disk membranes, absorbing around 440 nm in their protonated forms. In detergent micelles, we do not observe such peripheral Schiff bases, presumably as the free retinal is rapidly diluted and carried away from the protein in the large number of empty detergent micelles.

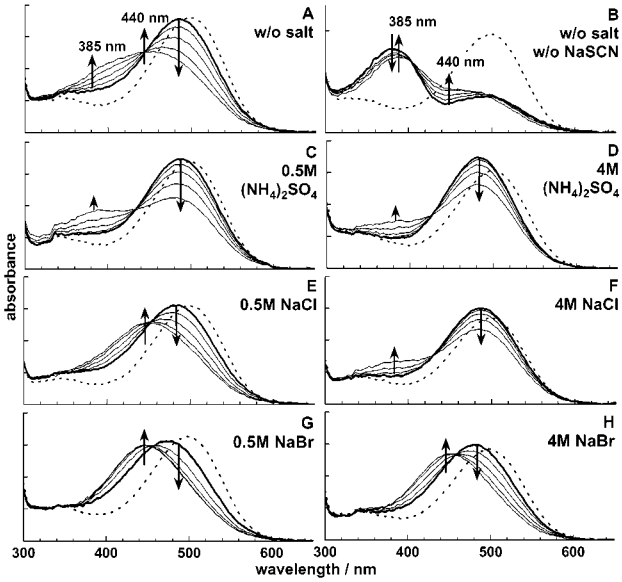

FIGURE 5: Influence of salts on the Meta II decay pathway. The decay pathway of Meta II was determined by UV−visible spectroscopy of purified rhodopsin in detergent (0.1% DM) at 20 °C and pH 3.5. Under these conditions, Meta II is in an anion dependent equilibrium between a form with deprotonated and with protonated Schiff base, Meta II_{380} and Meta II_{PSB}, absorbing at 380 nm (B) and 480 nm (A), respectively. For clarity, we added to all samples 10 mM NaSCN (except for B), which shifted the equilibrium entirely to the side of Meta II_{PSB} absorbing at 480 nm. Meta II_{PSB} (A) and Meta II_{380} (B) decay to both a 385 nm species via hydrolysis of the Schiff base and to a 440 nm species via denaturation of Meta II prior to Schiff base hydrolysis. Ammonium sulfate stabilizes the protein and shifts the decay pathway to the 385 nm species both at 0.5 (C) and 4 M concentration (D). Sodium chloride stabilizes only at 4 M concentration (F) and is destabilizing the protein at 0.5 M (E), where the 440 nm species is preferentially formed. Sodium bromide in the lower panel is destabilizing the protein both at 0.5 (G) and 4 M concentration (H), favoring as well the 440 nm decay product. In all panels, the broken line is the spectrum of the dark state before, the black thick line is the spectrum obtained immediately after sample illumination, subsequent spectra were recorded 2, 4, 8, and 16 min after illumination (thin lines). Arrows indicate the positions of the absorption maxima and the direction of absorption change.

pH 3.5 the protonation equilibrium entirely to the side of Meta II_{PSB} (Figure 5A). As evident from Figure 5A,B, the decay properties of Meta II_{380} are preserved in Meta II_{PSB} and we observe also with Meta II_{PSB} the parallel decay via the 385 and the 440 nm pathway, as indicated by arrows.

As evident from Figure 5C−H, the preference for either the 385 or the 440 nm pathway is strongly influenced by the presence of salts. While the kosmotrope ammonium sulfate generally prevents denaturation of Meta II and therefore favors formation of the 385 nm species (Figure 5C,D), the moderate chaotrope sodium bromide is rather destabilizing and favors formation of the 440 nm species (Figure 5G and H). Sodium chloride shows a very interesting behavior: At low salt concentration (0.5 M) we observe only formation of the 440 nm species, while at 4 M NaCl, only the 385 nm species is formed (Figure 5E,F). From these data, we can conclude that ammonium sulfate is stabilizing the retinal bound helix bundle of Meta II and prevents its denaturation prior to Schiff base hydrolysis. NaCl is destabilizing at low, but stabilizing at high concentrations, while NaBr is destabilizing at all concentrations, yet to a lesser extent at 4 M as compared to 0.5 M, as evident from the slowed spectral shift to 440 nm at 4 M. More chaotropic agents as NaSCN, guanidinium chloride, tetraethylammonium chloride, $CaCl_2$, and urea were found to be very destabilizing and to denature already the dark state of rhodopsin at 0.5 M (for NaSCN) or 4.0 M (for the others, spectra not shown).

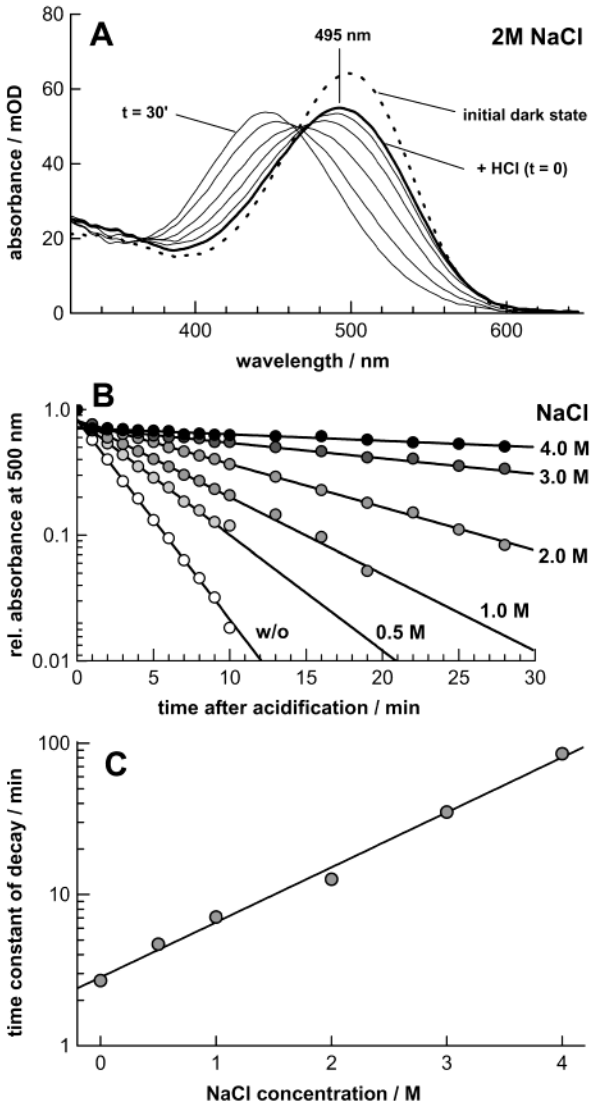

FIGURE 6: Influence of NaCl on the conformation of acid denatured rhodopsin. Rhodopsin in detergent (0.1% DM at 10 °C in 20 mM MOPS, pH 7.0) was acidified in the dark by addition of 1% (v/v) 10 M HCl (100 mM final) at $t = 0$ (thick line) and the subsequent spectral changes were followed at $t = 1$, 2, 4, 8, 16, and 30 min in the presence of 2 M NaCl (thin lines) (A). (B) Time course of the normalized absorbance decrease at 500 nm in the absence and in the presence of 0.5, 1.0, 2.0, 3.0, and 4.0 M NaCl, fitted to a negative exponential. (C) Time constant of the decay of the 500 nm absorbance as in panel B as a function of NaCl concentration.

Influence of Salts on the Stability of an Acid Denatured Loose Bundle State. Addition of 100 mM HCl (final pH ~1) to detergent solubilized unphotolyzed rhodopsin in the dark leads to a disintegration and denaturation of the dark state and formation of a 440 nm species (Figure 6). At 10 °C, the time constant of this decay to the 440 nm species is about 3 min in the absence of salt. This time constant increases steadily with increasing concentrations of sodium chloride up to 85 min at 4.0 M NaCl, as shown in Figure 6B,C.

The transition from the native dark state to the 440 nm species after acidification proceeds via a slightly blue-shifted

intermediate (λ_{max} 495 nm) with a reduced absorption coefficient (as compared to the native dark state), which is formed immediately after acidification and whose formation precedes the irreversible transition to the 440 nm species. This becomes obvious in the presence of NaCl as shown in Figure 6A, where this intermediate is selectively stabilized by 2 M NaCl, thereby slowing down the transition to the 440 nm species. In this 495 nm intermediate, most of the 60 nm opsin shift of the native dark state is retained. We can therefore conclude that the chromophore possesses still most of those tertiary contacts with the protein, which are responsible for the spectral tuning of the pigment absorption in the natively folded dark state. The small, ~5 nm deviation from the absorbance of the native dark state presumable reflects conformational changes within the protein due to acid induced protonation changes of amino acid side chain(s) of the protein. A possibly similar blue-shifted species with a reduced absorption coefficient was observed before as well at alkaline pH in the presence of 4 M KCl (*39*).

More chaotropic salts as $CaCl_2$ and NaBr fail to stabilize this 495 nm intermediate and yield a similar time constant of the transition to the 440 nm species as in the absence of salt (spectra not shown).

Influence of Salts on the Stability of the Native Dark State. To assess the influence of salts on the dark state, we used hydroxylamine as a probe for its stability. Hydroxylamine reacts with retinal Schiff bases readily to form retinal oxime (absorbing around 360 nm) and the free amino group. Reactivity of the Schiff base to hydroxylamine in rhodopsin and its photoproducts can therefore be a useful method to examine the accessibility of the retinal binding pocket for solvent molecules.

In the absence of salt, the dark state reacts only very slowly with hydroxylamine, and even at 50 °C the time constant of this chemical bleaching is still 87 min in the presence of 50 mM hydroxylamine at pH 7.0 in detergent (Figure 7 A). The hydroxylamine induced bleaching of the dark state accelerates considerably in the presence of sodium chloride, as shown in Figure 7B,C. In contrast to the previous experiments, sodium chloride is clearly destabilizing the native protein structure of the dark state over the entire concentration range. This acceleration is even more pronounced with more chaotropic salts as NaBr, $CaCl_2$, NaSCN, and NaTCA, which increase the reactivity of the Schiff base noticeably by favoring an unfolding of the compact structure of the dark state (Figure 7C). Sodium or magnesium sulfate, on the other hand, on the kosmotropic end of the Hofmeister series have no significant effect. Obviously, none of the examined salts slows down the rate constant of hydroxylamine bleaching, and the dark state therefore seems to have no pronounced susceptibility to kosmotropic salts. This is different, if we add sulfate and thiocyanate in combination. Under these conditions, sulfate may counteract the destabilizing effect of thiocyanate and increase the time constant of the decay by a factor of 4 (Figure 7C).

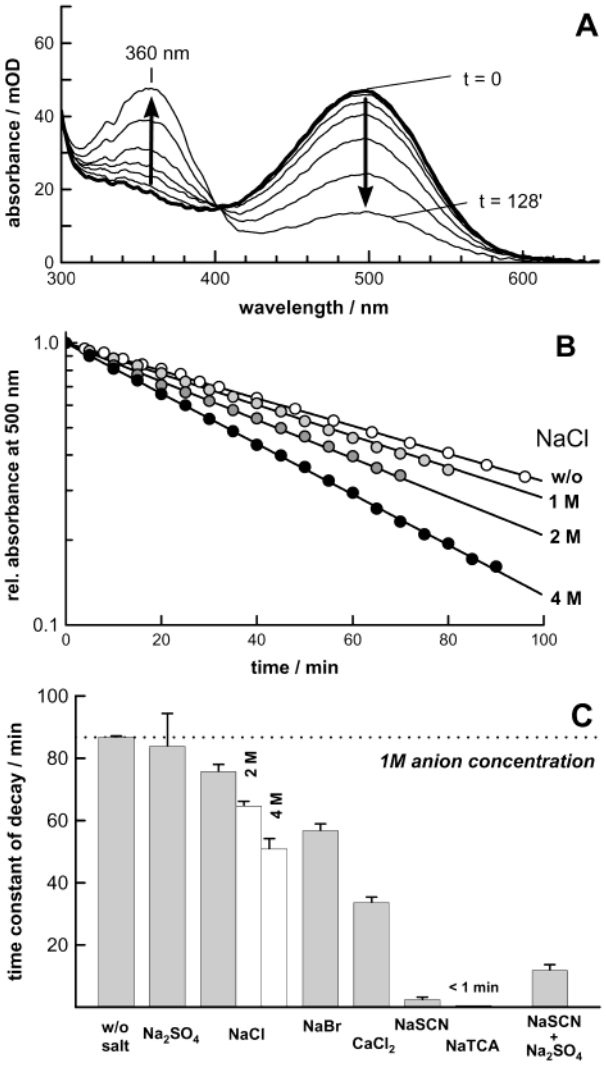

FIGURE 7: Influence of salts on the hydroxylamine reactivity of the Schiff base in the dark state. (A) The slow hydrolysis of the retinal chromophore of the dark state of rhodopsin (λ_{max} 500 nm) in detergent by the presence of 50 mM hydroxylamine was followed by UV−visible spectroscopy at pH 7.0 and 50 °C in the dark. Hydroxylamine attacks the retinal Schiff base and leads to the slow formation of free retinaloxime absorbing at 360 nm. The spectra in panel A were taken at $t = 0$, 4, 8, 16, 32, 64, and 128 min after the reaction was started, all in the absence of salt. (B) Time course of the absorbance decrease at 500 nm in the absence and in the presence of 1.0, 2.0, and 4.0 M NaCl. The straight lines are negative exponentials fitted to the normalized absorption at 500 nm (logarithmic scale). (C) Time constants of the decay of the dark state for different salts at 1 M anion concentration. In addition, the data of NaCl at 2.0 and 4.0 M are shown as well. To determine a putatively stabilizing effect of sulfate under otherwise destabilizing conditions, Na_2SO_4 and NaSCN were also assayed in combination (1 M each). The data are mean values ± SD of two experiments.

DISCUSSION

We have studied in this paper the stability of rhodopsin and its photoproduct states as a model system for α-helical membrane proteins. The unphotolyzed dark state of rhodopsin is remarkably stable toward high temperature and pH extremes, which is partly due to stabilizing interactions between the protein and the covalently bound 11-*cis* retinal chromophore. Light-dependent isomerization of the chromophore into the activating all-*trans* geometry abolishes many of these interactions and may therefore serve as a stability switch. We used this property and initiated protein unfolding by photolyzing rhodopsin under conditions, where the dark state is still stable, but its photoproducts are not.

We have examined the unfolding of these photoproduct states in the pH range from 2.0 to 9.0 at 30 °C and characterized in detail the structure of the resulting denatured

states. Important features of this states are (a) a UV−visible absorption peak at 440 or 370 nm at acidic or alkaline pH, respectively, indicating a partly solvent exposed chromophore lacking most of the tertiary contacts to the protein responsible for the opsin shifts in the native states, (b) an exposure of otherwise membrane embedded carboxylic acids from a weakly to a strongly hydrogen-bonding environment during the transition to the loose bundle, leading at alkaline pH to their partial deprotonation, (c) a large orientational change of the retinal chromophore during the transition to the denatured state, and (d) an increased fluorescence from intrinsic tryptophans, presumably indicating a reduced efficiency of energy transfer from these residues to the retinal chromophore. These tremendous changes in the spatial organization of the protein are, however, accompanied by only subtle changes in secondary structures as judged from the integrated intensity of the amide I difference bands (~1% of total integrated intensity of amide I bands).

These features indicate on one hand an almost complete preservation of the membrane spanning helices as secondary structural elements, but on the other hand a dramatic loss of tertiary contacts between these helices and between the helices and the chromophore. This suggests a picture, in which the helices form largely independent, membrane-spanning domains of secondary structure, which are possibly held together mainly by the spatial constraints imposed by the interconnecting loop-regions and by the lipid bilayer. From a structural point of view, this state may have some similarity with the molten globule state of soluble proteins, whose structural hallmarks are as well a considerable loss of tertiary contacts produced by tight packing of the protein side chains, despite of a pronounced conservation of secondary structure (*11*). Due to the fundamental structural differences between soluble and membrane proteins, this analogy should not be overstressed, and we rather describe this particular state as a loose helix bundle.

In contrast to soluble proteins, folding and assembly of membrane proteins take place under the physical constraint of the lipid bilayer, which limits the conformational space accessible to folding intermediates. For α-helical membrane proteins, the relatively simple view has emerged that single membrane spanning helices fold to some extent as separate entities and form relatively stable folding subdomains inserted into the membrane (*2*, *40*). These associate subsequently to form the correctly assembled membrane protein (*41*), which is stabilized by in part very specific electrostatic or packing interactions between helices, loops, cofactors, and lipids. In the case of retinal proteins, stabilizing effects were shown to be exerted both by connecting loops and by the retinal cofactor (*10*, *42*−*44*).

The concept of a loose bundle state as a denaturation product fits into this picture, and indeed, such a state may be a common intermediate found in the unfolding and possibly also the folding reactions of α-helical membrane proteins (*3*). It is a general observation for membrane proteins that unfolding reactions proceed with only limited changes in secondary structure (*4*). Studies on the structurally related membrane protein bacteriorhodopsin also revealed a large retention of secondary structure after denaturation as determined by IR (*45*) and CD spectroscopy (*46*), and by X-ray scattering (*47*). It was confirmed as well for the intramembraneous part of other membrane proteins (*48*, *49*). As compared to bacteriorhodopsin, the conservation of secondary structure during denaturation is even more pronounced in this study with rhodopsin. This possibly reflects the increased mean length of the connecting loops in the case of rhodopsin, allowing a loose structure of the helix bundle without the necessity of partial unfolding of helical termini.

In the second part of this study, we have investigated the influence of salts as cosolvents on the structural properties of the rhodopsin helix bundle and analyzed it in the framework of the Hofmeister effect. In the Hofmeister series, ions are classified as either kosmotropes (stabilizers) or chaotropes (destabilizers) according to their effect on protein properties. On a molecular level, kosmotropes, which are usually small or divalent ions with a high surface charge density, prevalently interact with water, but not with the protein (*50*). Chaotropes, on the other hand, are generally large monovalent ions, which interact less favorably with water and which preferentially bind to the less polar protein. The resulting balance between preferential exclusion from and preferential binding to the protein modifies the thermodynamic properties of the protein/solvent interface (*51*). The presence of kosmotropes, which are preferentially excluded from the interface, increases the interfacial tension between protein and solvent. The protein therefore tries to minimize its interfacial area by adopting a rather compact structure, corresponding in general to the native state. On the other hand, the presence of chaotropes, which preferentially bind in particular to the amide moiety of the unfolded protein backbone, favors an increase of this interfacial area. It is important to note, however, that a given salt always combines both chaotropic and kosmotropic aspects in its properties (*14*). In particular, chaotropic salts also have a kosmotropic component, as their presence increases the surface tension of the solvent, yet to a much smaller extent than do pure kosmotropes (*12*, *50*). The net effect of a salt on protein stability is therefore always the sum of its chaotropic and kosmotropic contributions acting in opposite directions.

One aim of this study was to obtain a detailed picture of the balance between the kosmotropic and the chaotropic contributions of salts on the stability of membrane proteins. We therefore varied the packing properties of the protein and examined (a) the dark state in its native fold, representing a protein with tight intramolecular packing and high overall stability, (b) the signaling state Meta II, with its reduced stability of the helix bundle, and (c) an entirely destabilized loose helix bundle, which was obtained after acid denaturation of rhodopsin. For simplicity, we restricted this second part of our study to solubilized rhodopsin in detergent micelles.

We found that the ion selectivity of salt-dependent stabilization or destabilization of the protein follows the Hofmeister series conclusively in all three examples. Specifically, we observed that kosmotropic salts favor a native or nativelike fold of the protein, while a non-native, denatured fold is favored in the presence of chaotropes. Yet the null-point in the Hofmeister series, which divides stabilizers from destabilizers, was different in all three examples. This could be clearly shown by analyzing the respective effect of sodium chloride, which constitutes an intermediate salt in the sense of the Hofmeister series. In the experiments on the hydroxylamine reactivity of the dark state of rhodopsin with its particular stability, sodium chloride was found to be desta-

bilizing at all examined concentrations. A clearly different picture was obtained for the loose helix bundle being formed after acid denaturation of rhodopsin. With this protein state, we observed a stabilization of a more nativelike tertiary structure by sodium chloride at any tested concentration, indicating an increased sensitivity of the protein in this state for the kosmotropic rather than the chaotropic effect of salts. Finally, in the example of intermediate stability, the Meta II photoproduct state, sodium chloride was found to be destabilizing at low and stabilizing at high concentrations.

Obviously, with decreasing stability, the protein's susceptibility for the kosmotropic effect increases, presumably because native helix−helix and helix−retinal contacts are enhanced by the lateral pressure component of the salt dependent increase of the interfacial tension of the protein/solvent interface. In the case of the acid denatured loose bundle state, this led to the stabilization of an unfolding intermediate, in which important native-like contacts between protein and chromophore were restored. The net property of a salt in terms of stabilization/destabilization therefore depends also on the structural properties of the studied protein conformation. In particular, switching from a tightly packed native state to a highly destabilized state may result in a shift of the null point between stabilization and destabilization in the Hofmeister series to more chaotropic ions.

ACKNOWLEDGMENT

We thank B. Mayer, W. Sevenich, K. Zander, and P. Merkt for their invaluable technical assistance.

REFERENCES

1. Wallin, E., and von Heijne, G. (1998) *Protein Sci. 7*, 1029−1038.
2. White, S. H., and Wimley, W. C. (1999) *Annu. Rev. Biophys. Biomol. Struct. 28*, 319−365.
3. Booth, P. J., and Curran, A. R. (1999) *Curr. Opin. Struct. Biol. 9*, 115−121.
4. Stowell, M. H., and Rees, D. C. (1995) *Adv. Protein Chem. 46*, 279−311.
5. Vogel, R., and Siebert, F. (2000) *Curr. Opin. Chem. Biol. 4*, 518−523.
6. Menon, S. T., Han, M., and Sakmar, T. P. (2001) *Physiol. Rev. 81*, 1659−1688.
7. Shichida, Y., and Imai, H. (1998) *Cell. Mol. Life Sci. 54*, 1299−1315.
8. Siebert, F. (1995) *Israel. J. Chem. 35*, 309−323.
9. Palczewski, K., Kumasaka, T., Hori, T., Behnke, C. A., Motoshima, H., Fox, B. A., Le Trong, I., Teller, D. C., Okada, T., Stenkamp, R. E., Yamamoto, M., and Miyano, M. (2000) *Science 289*, 739−745.
10. Cladera, J., Galisteo, M. L., Sabes, M., Mateo, P. L., and Padros, E. (1992) *Eur. J. Biochem. 207*, 581−585.
11. Arai, M., and Kuwajima, K. (2000) *Adv. Protein Chem. 53*, 209−282.
12. Collins, K. D., and Washabaugh, M. W. (1985) *Q. Rev. Biophys. 18*, 323−422.
13. Cacace, M. G., Landau, E. M., and Ramsden, J. J. (1997) *Q. Rev. Biophys. 30*, 241−277.
14. Baldwin, R. L. (1996) *Biophys. J. 71*, 2056−2063.
15. Hofmeister, F. (1888) *Arch. Exp. Pathol. Pharmakol. 24*, 247−260.
16. Vogel, R., and Siebert, F. (2002) *Biochemistry 41*, 3529−3535.
17. Dér, A., and Ramsden, J. J. (1998) *Naturwissenschaften 85*, 353−355.
18. Neagu, A., Neagu, M., and Dér, A. (2001) *Biophys. J. 81*, 1285−1294.
19. Vogel, R., Fan, G. B., Sheves, M., and Siebert, F. (2000) *Biochemistry 39*, 8895−8908.
20. Vogel, R., Fan, G. B., Sheves, M., and Siebert, F. (2001) *Biochemistry 40*, 483−493.
21. Ganter, U. M., Schmid, E. D., Perez-Sala, D., Rando, R. R., and Siebert, F. (1989) *Biochemistry 28*, 5954−5962.
22. DeGrip, W. J. (1982) *Methods Enzymol. 81*, 197−207.
23. Vogel, R., Fan, G. B., Siebert, F., and Sheves, M. (2001) *Biochemistry 40*, 13342−13352.
24. Vogel, R., and Siebert, F. (2001) *J. Biol. Chem. 276*, 38487−38493.
25. Kochendoerfer, G. G., Lin, S. W., Sakmar, T. P., and Mathies, R. A. (1999) *Trends Biochem. Sci. 24*, 300−305.
26. Blatz, P. E., Mohler, J. H., and Navangul, H. V. (1972) *Biochemistry 11*, 848−855.
27. Livnah, N., and Sheves, M. (1993) *J. Am. Chem. Soc. 115*, 351−353.
28. Rothschild, K. J., Cantore, W. A., and Marrero, H. (1983) *Science 219*, 1333−1335.
29. Rath, P., DeCaluwe, L. L., Bovee-Geurts, P. H., DeGrip, W. J., and Rothschild, K. J. (1993) *Biochemistry 32*, 10277−10282.
30. Fahmy, K., Jäger, F., Beck, M., Zvyaga, T. A., Sakmar, T. P., and Siebert, F. (1993) *Proc. Natl. Acad. Sci. U.S.A. 90*, 10206−10210.
31. Beck, M., Siebert, F., and Sakmar, T. P. (1998) *FEBS Lett. 436*, 304−308.
32. Isele, J., Sakmar, T. P., and Siebert, F. (2000) *Biophys. J. 79*, 3063−3071.
33. Jäger, F., Fahmy, K., Sakmar, T. P., and Siebert, F. (1994) *Biochemistry 33*, 10878−10882.
34. Chabre, M., and Breton, J. (1979) *Vision Res. 19*, 1005−1018.
35. Ebrey, T. G. (1972) *Photochem. Photobiol. 15*, 585−588.
36. Farrens, D. L., and Khorana, H. G. (1995) *J. Biol. Chem. 270*, 5073−5076.
37. DeGrip, W. J. (1982) *Methods Enzymol. 81*, 256−265.
38. Sakamoto, T., and Khorana, H. G. (1995) *Proc. Natl. Acad. Sci. U.S.A. 92*, 249−253.
39. Koutalos, Y. (1992) *Biophys. J. 61*, 272−275.
40. Popot, J. L., and Engelman, D. M. (2000) *Annu. Rev. Biochem. 69*, 881−922.
41. Ridge, K. D., Lee, S. S., and Yao, L. L. (1995) *Proc. Natl. Acad. Sci. U.S.A. 92*, 3204−3208.
42. Kim, J. M., Booth, P. J., Allen, S. J., and Khorana, H. G. (2001) *J. Mol. Biol. 308*, 409−422.
43. Kahn, T. W., Sturtevant, J. M., and Engelman, D. M. (1992) *Biochemistry 31*, 8829−8839.
44. Landin, J. S., Katragadda, M., and Albert, A. D. (2001) *Biochemistry 40*, 11176−11183.
45. Taneva, S. G., Caaveiro, J. M., Muga, A., and Goni, F. M. (1995) *FEBS Lett. 367*, 297−300.
46. Brouillette, C. G., Muccio, D. D., and Finney, T. K. (1987) *Biochemistry 26*, 7431−7438.
47. Müller, J., Münster, C., and Salditt, T. (2000) *Biophys. J. 78*, 3208−3217.
48. Grinberg, A. V., Gevondyan, N. M., Grinberg, N. V., and Grinberg, V. Y. (2001) *Eur. J. Biochem. 268*, 5027−5036.
49. Haltia, T., Semo, N., Arrondo, J. L., Goni, F. M., and Freire, E. (1994) *Biochemistry 33*, 9731−9740.
50. Collins, K. D. (1995) *Proc. Natl. Acad. Sci. U.S.A. 92*, 5553−5557.
51. Timasheff, S. N. (1998) *Adv. Protein Chem. 51*, 355−432.

BI016024F